Single-junction quantum-circuit refrigerator

Single-junction quantum-circuit refrigerator

Cite as: AIP Advances **12**, 075005 (2022); https://doi.org/10.1063/5.0096849
Submitted: 22 April 2022 • Accepted: 02 June 2022 • Published Online: 01 July 2022

V. Vadimov, A. Viitanen, T. Mörstedt, et al.

Single-junction quantum-circuit refrigerator

Cite as: AIP Advances 12, 075005 (2022); doi: 10.1063/5.0096849
Submitted: 22 April 2022 • Accepted: 2 June 2022 •
Published Online: 1 July 2022

V. Vadimov,[1,2,a] A. Viitanen,[1] T. Mörstedt,[1] T. Ala-Nissila,[2,3] and M. Möttönen[1,4]

AFFILIATIONS

[1] QCD Labs, QTF Centre of Excellence, Department of Applied Physics, Aalto University, P.O. Box 13500, FI-00076 Aalto, Espoo, Finland
[2] MSP Group, QTF Centre of Excellence, Department of Applied Physics, Aalto University, P.O. Box 11000, FI-00076 Aalto, Espoo, Finland
[3] Interdisciplinary Centre for Mathematical Modelling, Department of Mathematical Sciences, Loughborough University, Loughborough LE11 3TU, United Kingdom
[4] VTT Technical Research Centre of Finland Ltd., QTF Center of Excellence, P.O. Box 1000, FI-02044 VTT, Finland

[a] **Author to whom correspondence should be addressed:** vasilii.1.vadimov@aalto.fi

ABSTRACT

We propose a quantum-circuit refrigerator (QCR) based on photon-assisted quasiparticle tunneling through a single normal-metal–insulator–superconductor (NIS) junction. In contrast to previous studies with multiple junctions and an additional charge island for the QCR, we directly connect the NIS junction to an inductively shunted electrode of a superconducting microwave resonator making the device immune to low-frequency charge noise. At low characteristic impedance of the resonator and parameters relevant to a recent experiment, we observe that a semiclassical impedance model of the NIS junction reproduces the bias voltage dependence of the QCR-induced damping rate and frequency shift. For high characteristic impedances, we derive a Born–Markov master equation and use it to observe significant non-linearities in the QCR-induced dissipation and frequency shift. We further demonstrate that, in this regime, the QCR can be used to initialize the linear resonator into a non-thermal state even in the absence of any microwave drive.

I. INTRODUCTION

Superconducting quantum circuits[1–4] have emerged as a highly promising platform for quantum simulations and quantum information processing. As these circuits advance in terms of performance and complexity, active control of individual devices within the circuit constitutes a key challenge. In particular, the control of temperature and dissipation in devices such as transmission lines,[5] microwave resonators,[6] or qubits[7–11] enables targeted cooling and initialization of these devices. This has already been achieved with the invention of the quantum-circuit refrigerator (QCR),[12] a stand-alone, on-chip device that can locally cool superconducting circuits based on photon-assisted tunneling utilizing a pair of parallel normal-metal–insulator–superconductor (NIS) junctions.[13,14] We note that the NIS junctions have been widely used for refrigeration of electronic subsystem[15–19] due to the non-linear Peltier effect predicted in Ref. 20. Contrary to this, the QCR cools down the photonic degrees of freedom of the system.

In this work, we present a simplified quantum-circuit refrigerator based on a single NIS junction and analyze this device in the case of direct coupling to a coplanar waveguide (CPW) resonator. The basic operation principle is similar to that of a double-junction refrigerator: A small bias voltage $V_0 < \Delta/e$, where Δ is the superconductor gap parameter, is applied across the junction. Quasiparticles can tunnel through the insulating barrier, energetically allowed by absorption of photons from the coupled circuit, which decreases the temperature of the electric degrees of freedom of the circuit.[14,21,22] Such tunneling events induce quantum–state transitions, for example, in a microwave resonator.[6,23] With increasing voltages $V_0 > \Delta/e$, photon emission rate into the circuit approaches that of photon absorption, which leads to heating.[24,25] Therefore, we operate the QCR in the range $\Delta - \hbar\,\omega_r < eV_0 < \Delta$, where ω_r is the angular frequency of the lowest mode of the circuit.

We first present the design of a single-junction QCR coupled to a resonator, compare it to conventional double-junction

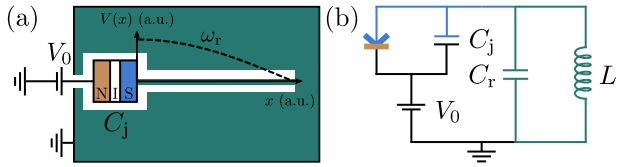

FIG. 1. (a) Design of a single-junction QCR directly connected to a $\lambda/4$ CPW resonator. The voltage profile of the fundamental mode at angular frequency ω_r has an anti-node at the superconductor lead and a node where the center conductor connects to the ground plane (green). The NIS junction of capacitance C_j is biased with a voltage V_0 applied to the normal-metal lead. (b) Lumped-element circuit model of the fundamental resonator mode coupled to the NIS junction.

microcooler devices, and analyze this system in terms of its tunable Lamb shift and dissipation rate. We further investigate the case of a single-junction QCR coupled to a high-impedance resonator, including multi-photon processes. Finally, we present our conclusions and explore further theoretical and experimental opportunities with this device.

II. SYSTEM SETUP

The system under study in Fig. 1 consists of a single normal-metal–insulator–superconductor tunnel junction connected to a superconducting resonator forming a direct conduction path from the junction to the ground potential. The normal-metal lead is used to voltage bias the junction, providing on-demand control of tunneling. This novel implementation of a QCR differs from the previous devices[12] in two ways. First, we employ a single NIS junction as opposed to a double junction in a SINIS structure. Second, we avoid forming a charge island between the junction and the resonator by directly connecting the resonator to the NIS junction as opposed to capacitive coupling. The primary advantage of this approach is to mitigate low-frequency charge noise caused by changes in the charge state of the island and the charge traps in its vicinity.[26]

To achieve an equal tunneling rate and cooling power as for the double-junction device,[12,14] the corresponding single-junction QCR can be designed with half the tunneling resistance. In an experimental setting, the single-junction QCR can be controlled with a single line, whereas the double-junction QCR is typically operated through two separate control lines, an input and an output line.[6,12,27] For the single-junction QCR, a directly connected $\lambda/4$ CPW resonator naturally fixes the superconducting electrode to the ground potential at low frequencies.

III. SEMICLASSICAL MODEL

We begin with an analysis of the dissipation and frequency shifts induced by the coupling of the resonator to the NIS junction. To this end, we employ classical equations of motion for the electromagnetic field in the circuit. The current–voltage characteristic of an NIS junction is both strongly non-linear and non-local in time. However, if we assume the ac component of the voltage to be small, we can replace the junction by an effective frequency-dependent conductance, which can be controlled by the dc component of the voltage. To proceed, we define

$$V_{\mathrm{NIS}}(t) = V_{\mathrm{dc}} + \frac{1}{2\pi}\int_{-\infty}^{+\infty} V_{\mathrm{ac}}(\omega)\mathrm{e}^{-\mathrm{i}\omega t}\, d\omega, \tag{1}$$

$$I_{\mathrm{NIS}}(t) \approx I_{\mathrm{dc}}(V_{\mathrm{dc}}) + \frac{1}{2\pi}\int_{-\infty}^{+\infty} G_{\mathrm{NIS}}(V_{\mathrm{dc}},\omega)V_{\mathrm{ac}}(\omega)\mathrm{e}^{-\mathrm{i}\omega t}\, d\omega, \tag{2}$$

where $G(V_{\mathrm{dc}},\omega)$ is the conductance of the junction at bias voltage V_{dc} and angular frequency ω. Such an expansion is valid in the limit[28] $|eV_{\mathrm{ac}}(\omega)| \ll |\hbar\omega|$.

To find the dissipation rate and the Lamb shift of the resonator caused by the coupling to the NIS junction, we write Kirchhoff's law for the circuit shown in Fig. 1(b) as

$$I_{\mathrm{NIS}}[V_0 - \dot{\varphi}] = C\ddot{\varphi} + \frac{\varphi}{L}, \tag{3}$$

where $C = C_j + C_r$,

$$\varphi(t) = \int_{-\infty}^{t} V(t')\, \mathrm{d}t', \tag{4}$$

and $V(t)$ is the voltage across the capacitance C_r. Employing Eq. (2) and going to the Fourier picture, we obtain an equation for the eigenfrequency of the resonator as follows:

$$-\omega^2 C - \mathrm{i}\omega G_{\mathrm{NIS}}(V_0,\omega) + \frac{1}{L} = 0. \tag{5}$$

Provided the conductance is small $G_{\mathrm{NIS}}(V_0,\omega) \ll Z_r^{-1}$ and changes smoothly on the frequency scale of $G_{\mathrm{NIS}}(V_0,\omega_r)Z_r\omega_r$, where $Z_r = \sqrt{L/C}$ is the characteristic impedance of the resonator, we can find the angular-frequency shift ω_L and the dissipation rate γ as

$$\omega_L - \mathrm{i}\gamma \approx -\frac{\mathrm{i}}{2}G_{\mathrm{NIS}}(V_0,\omega_r)\omega_r Z_r, \tag{6}$$

where $\omega_r = 1/\sqrt{LC}$ is the resonance frequency of the bare LC circuit. Thus, both of these quantities are proportional to the imaginary and real parts of the NIS junction conductance. We can use this simple approach when the voltage across the capacitor satisfies the condition $|eV(\omega)| \ll |\hbar\omega|$. In the quantum regime, voltage fluctuations are bounded from below by zero point fluctuations, $\delta V(\omega)/|\omega| \sim \sqrt{\hbar Z_r/2}$. Thus, we obtain the applicability criterion for our result to be $\sqrt{\pi Z_r/R_K} \ll 1$, where $R_K = 2\pi\hbar/e^2$ is the von Klitzing constant.

Following Ref. 28, we derive the real and imaginary parts of the junction conductance and obtain the following expressions:

$$\begin{aligned} &Re[G_{\mathrm{NIS}}(V_0,\omega)] \\ &= \frac{1}{8R_j\omega}\int_{-\infty}^{+\infty} \mathrm{Im}\left[\frac{\hbar\omega' + \mathrm{i}\gamma_D\Delta}{\sqrt{\Delta^2 - (\hbar\omega' + \mathrm{i}\gamma_D\Delta)^2}}\right] \\ &\times\left\{\tanh\left[\frac{\hbar(\omega'+\omega) - eV_0}{2k_BT}\right] + \tanh\left[\frac{\hbar(\omega'+\omega) + eV_0}{2k_BT}\right]\right. \\ &\left. - \tanh\left[\frac{\hbar(\omega'-\omega) - eV_0}{2k_BT}\right] - \tanh\left[\frac{\hbar(\omega'-\omega) + eV_0}{2k_BT}\right]\right\} \mathrm{d}\omega', \end{aligned} \tag{7}$$

$$\begin{aligned}\mathrm{Im}[G_{\mathrm{NIS}}(V_0,\omega)] &= \frac{1}{4R_\mathrm{j}\omega}\int_{-\infty}^{+\infty} Re\left[\frac{\hbar\omega' + \mathrm{i}\gamma_\mathrm{D}\Delta}{\sqrt{\Delta^2-(\hbar\omega'+\mathrm{i}\gamma_\mathrm{D}\Delta)^2}}\right] \\ &\times\left(\frac{1}{2}\left\{\tanh\left[\frac{\hbar(\omega'+\omega)-eV_0}{2k_\mathrm{B}T}\right]+\tanh\left[\frac{\hbar(\omega'+\omega)+eV_0}{2k_\mathrm{B}T}\right]\right.\right. \\ &+\tanh\left[\frac{\hbar(\omega'-\omega)-eV_0}{2k_\mathrm{B}T}\right]+\left.\left.\tanh\left[\frac{\hbar(\omega'-\omega)+eV_0}{2k_\mathrm{B}T}\right]\right\}\right. \\ &-\left.\tanh\left[\frac{\hbar\omega'-eV_0}{2k_\mathrm{B}T}\right]-\tanh\left[\frac{\hbar\omega'+eV_0}{2k_\mathrm{B}T}\right]\right)\mathrm{d}\omega', \end{aligned} \tag{8}$$

where R_j is the junction resistance in the normal state, γ_D is the Dynes parameter of the junction, and T is the electron temperature of the normal metal. The frequency shift and the dissipation rate of the resonator are shown in Fig. 2 for parameters corresponding to the experiments in Ref. 27, where a double-junction QCR capacitively coupled to a $\lambda/2$ resonator is employed. The theoretical results from Eqs. (6)–(8) well agree with the experimental data despite the differences in the design of the sample and our model. Such a good correspondence can be explained by the fact that the frequency shift and the dissipation rate are both proportional to the sum of the conductances of the NIS junctions in the QCR. Provided that the SINIS junction is symmetric, the expressions for the frequency shift and the dissipation rate coincide with Eq. (6), where the tunneling resistance and the characteristic impedance are adjusted accordingly. However, for the asymmetric junction, this statement is no longer valid since the voltages across the insulating layers of the SINIS junction are not equal to each other in this case.

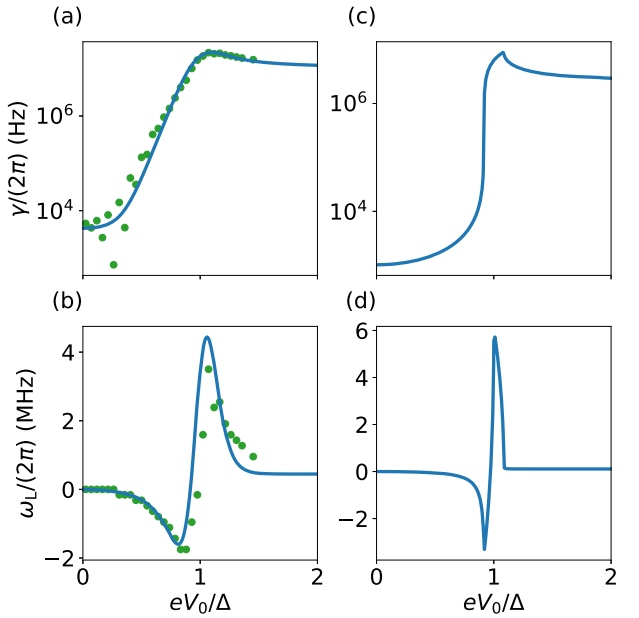

FIG. 2. (a) QCR-induced dissipation rate and (b) frequency shift of a CPW resonator as functions of the bias voltage of the NIS junction. Blue lines correspond to Eqs. (6)–(8), and the green dots show the experimental data from Ref. 27. The QCR-induced frequency shift is defined to vanish at zero voltage $V = 0$. The device parameters are given by $\omega_\mathrm{r} = 2\pi \times 4.67$ GHz, $Z_\mathrm{r} = 34.8$ Ω, $\Delta = 0.215$ meV, $T = 0.17$ K, $\gamma_\mathrm{D} = 4 \times 10^{-4}$, and the junction resistance $R_\mathrm{j} = 16$ kΩ is obtained from a fit to the experimental relaxation rate. Panels (c) and (d) show the dissipation rate and the frequency shift, respectively, for identical parameters except for $T = 0$ K. The positions of the dips and peaks in the frequency shifts are determined by $eV_0 = \Delta, \Delta \pm \hbar\omega_\mathrm{r}$.

IV. QUANTUM MODEL

If the condition $\sqrt{\pi Z_\mathrm{r}/R_\mathrm{K}} \ll 1$ is violated, multi-photon processes become important in the quantum limit. In this case, we need to quantize the electromagnetic field in the circuit. Employing the standard field quantization approach,[23] we obtain the following Hamiltonian for the circuit:

$$\hat{H} = \hat{H}_\mathrm{r} + \hat{H}_\mathrm{NS} + \hat{H}_\mathrm{t}, \tag{9}$$

$$\hat{H}_\mathrm{r} = \frac{\hat{q}^2}{2C} + \frac{\hat{\varphi}^2}{2L}, \tag{10}$$

$$\hat{H}_\mathrm{NS} = \sum_{k\sigma}\left(\xi_k^\mathrm{n} - eV_0\right)\hat{d}_{k\sigma}^\dagger\hat{d}_{k\sigma} + \sum_{p\sigma}\xi_p^\mathrm{s}\hat{c}_{p\sigma}^\dagger\hat{c}_{p\sigma} + \Delta\sum_p\left(\hat{c}_{p\uparrow}\hat{c}_{\bar{p}\downarrow} + \mathrm{h.c.}\right), \tag{11}$$

$$\hat{H}_\mathrm{t} = \sum_{kp\sigma}\left(\Gamma_{kp}\hat{d}_{k\sigma}^\dagger\hat{c}_{p\sigma}\mathrm{e}^{\mathrm{i}\frac{e\hat{\varphi}}{\hbar}} + \mathrm{h.c.}\right), \tag{12}$$

where $\hat{\varphi}$ and $\hat{q}$ are the canonically conjugate $[\hat{\varphi},\hat{q}] = \mathrm{i}\hbar$ flux and charge operators of the LC circuit, respectively, $\hat{d}_{k\sigma}$ is the annihilation operator of an electron in mode k with spin projection σ in the normal metal, ξ_k^n is the energy of this mode with respect to the Fermi energy, $\hat{c}_{p\sigma}$ is the annihilation operator of an electron in the mode p with spin projection σ in the superconductor, ξ_p^s is the energy of this mode with respect to the Fermi energy, and Γ_{kp} is the tunneling matrix element. We emphasize that the coupling between the electromagnetic and fermionic degrees of freedom occurs through the charge shift operator $\exp(\mathrm{i}e\hat{\varphi}/\hbar)$ in the tunneling Hamiltonian, since the tunneling of an electron through the junction is associated with a change in the capacitor charge by a single elementary charge. Introducing the notations

$$\hat{a} = \frac{1}{\sqrt{2\hbar Z_\mathrm{r}}}(\hat{\varphi} + \mathrm{i}Z_\mathrm{r}\hat{q}),\ \alpha = e\sqrt{\frac{Z_\mathrm{r}}{2\hbar}} = \sqrt{\frac{\pi Z_\mathrm{r}}{R_\mathrm{K}}}, \tag{13}$$

$$\hat{F} = \mathrm{e}^{\mathrm{i}\alpha\left(\hat{a}+\hat{a}^\dagger\right)},\ \hat{\Theta} = \sum_{kp\sigma}\Gamma_{kp}\hat{d}_{k\sigma}^\dagger\hat{c}_{p\sigma}, \tag{14}$$

and employing the standard Born–Markov approximation, we obtain a Redfield master equation[29] that governs the dynamics of the resonator density operator $\hat{\rho}$ as

$$\frac{\mathrm{d}\hat{\rho}}{\mathrm{d}t} = \mathscr{L}(\hat{\rho}) = -\frac{\mathrm{i}}{\hbar}\left[\hat{H}_{\mathrm{r}}, \hat{\rho}\right] - \frac{1}{\hbar^2}\int_0^{+\infty} \Big\{\Big[\hat{F}\hat{F}^\dagger(-\tau)\hat{\rho} - \hat{F}^\dagger(-\tau)\hat{\rho}\hat{F}\Big]\Big\langle\hat{\Theta}^\dagger(\tau)\hat{\Theta}\Big\rangle + \Big[\hat{\rho}\hat{F}^\dagger(-\tau)\hat{F} - \hat{F}\hat{\rho}\hat{F}^\dagger(-\tau)\Big]\Big\langle\hat{\Theta}\hat{\Theta}^\dagger(\tau)\Big\rangle + \Big[\hat{F}^\dagger\hat{F}(-\tau)\hat{\rho} - \hat{F}(-\tau)\hat{\rho}\hat{F}^\dagger\Big]\Big\langle\hat{\Theta}(\tau)\hat{\Theta}^\dagger\Big\rangle + \Big[\rho\hat{F}(-\tau)\hat{F}^\dagger - \hat{F}^\dagger\hat{\rho}\hat{F}(-\tau)\Big]\Big\langle\hat{\Theta}^\dagger\hat{\Theta}(\tau)\Big\rangle\Big\}\,\mathrm{d}\tau, \quad (15)$$

where $\mathscr{L}$ is the Liouvillian of the system, and the time-dependent operators are given in the interaction picture,

$$\hat{F}(\tau) = \mathrm{e}^{\mathrm{i}\frac{\hat{H}_{\mathrm{r}}\tau}{\hbar}}\hat{F}\mathrm{e}^{-\mathrm{i}\frac{\hat{H}_{\mathrm{r}}\tau}{\hbar}}, \quad \hat{\Theta}(\tau) = \mathrm{e}^{\mathrm{i}\frac{\hat{H}_{\mathrm{NS}}\tau}{\hbar}}\hat{\Theta}\,\mathrm{e}^{-\mathrm{i}\frac{\hat{H}_{\mathrm{NS}}\tau}{\hbar}}. \quad (16)$$

In the following, we derive a convenient form for the dynamical correlators of the electron tunneling operator:

$$\Big\langle\hat{\Theta}^\dagger(\tau)\hat{\Theta}\Big\rangle = \sum_{kp\sigma}|\Gamma_{kp}|^2\Big\langle\hat{d}_{k\sigma}(\tau)\hat{d}^\dagger_{k\sigma}\Big\rangle\Big\langle\hat{c}^\dagger_{p\sigma}(\tau)\hat{c}_{p\sigma}\Big\rangle \approx 2|\Gamma|^2\sum_k\Big\langle\hat{d}_{k\uparrow}(\tau)\hat{d}^\dagger_{k\uparrow}\Big\rangle\sum_p\Big\langle\hat{c}^\dagger_{p\uparrow}(\tau)\hat{c}_{p\uparrow}\Big\rangle. \quad (17)$$

Here, we assume that the tunneling matrix elements have equal magnitudes $|\Gamma_{kp}|^2 = |\Gamma|^2$ regardless of the spatial structure of the normal modes k and p. We carry out the quantum-mechanical averaging assuming thermal states are described by Fermi–Dirac distributions of the quasiparticles in the superconductor and shifted by the bias voltage in the normal metal as

$$\Big\langle\hat{d}_{k\uparrow}(\tau)\hat{d}^\dagger_{k\uparrow}\Big\rangle = \frac{\exp\left[-\frac{i}{\hbar}(\xi^{\mathrm{n}}_k - eV_0)\tau\right]}{1+\exp\left[-\frac{\xi^{\mathrm{n}}_k}{k_{\mathrm{B}}T}\right]}, \quad (18)$$

$$\Big\langle\hat{c}^\dagger_{p\uparrow}(\tau)\hat{c}_{p\uparrow}\Big\rangle = \frac{\exp\left(\frac{i}{\hbar}\varepsilon_p\tau\right)}{2\left[1+\exp\left(\frac{\varepsilon_p}{k_{\mathrm{B}}T}\right)\right]}\left(1+\frac{\xi^{\mathrm{s}}_p}{\varepsilon_p}\right) + \frac{\exp\left(-\frac{i}{\hbar}\varepsilon_p\tau\right)}{2\left[1+\exp\left(-\frac{\varepsilon_p}{k_{\mathrm{B}}T}\right)\right]}\left(1-\frac{\xi^{\mathrm{s}}_p}{\varepsilon_p}\right), \quad (19)$$

where $\varepsilon_p = \sqrt{\left(\xi^{\mathrm{s}}_p\right)^2 + \Delta^2}$. The summation over the normal electronic modes of the normal metal k and the superconductor p can be replaced with integration over the normal electron energy ξ^{n}_k and ξ^{s}_p, respectively, multiplied by the corresponding density of states as

$$\sum_{k(p)}X_{k(p)} = \mathcal{V}_{\mathrm{n(s)}}\int_{-\infty}^{+\infty}\nu_{\mathrm{n(s)}}\left(\xi^{\mathrm{n(s)}}_{k(p)}\right)X\left(\xi^{\mathrm{n(s)}}_{k(p)}\right)\,\mathrm{d}\xi^{\mathrm{n(s)}}_{k(p)}, \quad (20)$$

where X may be replaced by the corresponding correlators, $\mathcal{V}_{\mathrm{n(s)}}$ is the volume of the normal metal (superconductor), and $\nu_{\mathrm{n(s)}}\left(\xi^{\mathrm{n(s)}}_{k(p)}\right)$ is the density of states per the unit volume per spin projection of the normal metal (superconductor).

Only the electronic states close to the Fermi level, where the density of states is approximately constant, give a significant contribution to the tunneling correlation function. Contribution of the levels that lie far away from the Fermi energy is negligible and we may assume that the density of states is an arbitrary function, which decays at high energies in order to ensure the convergence of the corresponding integral. Thus, we employ a Gaussian ansatz for the density of states,

$$\nu_{\mathrm{n(s)}}\left(\xi^{\mathrm{n(s)}}_{k(p)}\right) = \nu^{(0)}_{\mathrm{n(s)}}\,\exp\left[-\left(\frac{\xi^{\mathrm{n(s)}}_{k(p)}}{\hbar\Omega}\right)^2\right], \quad (21)$$

where the cut-off energy $\hbar\Omega \gg \Delta, eV_0$ defines the highest energy scale of the NIS junction. After integration over $\xi^{\mathrm{n(s)}}_{k(p)}$, we obtain the expressions for the dynamical correlation functions of the electronic tunneling operator $\hat{\Theta}$ as

$$\Big\langle\hat{\Theta}^\dagger(\tau)\hat{\Theta}\Big\rangle = \frac{2R_{\mathrm{K}}\hbar^2}{R_{\mathrm{j}}}g^{>}_{\mathrm{n}}(\tau)g^{<}_{\mathrm{s}}(-\tau)\mathrm{e}^{\mathrm{i}\frac{eV_0}{\hbar}\tau}, \quad (22)$$

$$\Big\langle\hat{\Theta}\hat{\Theta}^\dagger(\tau)\Big\rangle = \frac{2R_{\mathrm{K}}\hbar^2}{R_{\mathrm{j}}}g^{<}_{\mathrm{n}}(\tau)g^{>}_{\mathrm{s}}(-\tau)\mathrm{e}^{\mathrm{i}\frac{eV_0}{\hbar}\tau}, \quad (23)$$

where the resistance of the junction is given by

$$R_{\mathrm{j}} = \frac{R_{\mathrm{K}}}{4\pi^2|\Gamma|^2\nu^{(0)}_{\mathrm{n}}\nu^{(0)}_{\mathrm{s}}\mathcal{V}_{\mathrm{n}}\mathcal{V}_{\mathrm{s}}}, \quad (24)$$

and the quasiclassical greater and lesser Green's functions of the normal metal and the superconductor assume the forms

$$g^{>(<)}_{\mathrm{n(s)}}(\tau) = \frac{1}{2\pi}\int g^{>(<)}_{\mathrm{n(s)}}(\omega)\mathrm{e}^{-i\omega\tau}\,d\omega, \quad (25)$$

$$g^{>(<)}_{\mathrm{n}}(\omega) = \frac{\exp\left(-\frac{\omega^2}{\Omega^2}\right)}{1+\exp\left(\mp\frac{\hbar\omega}{k_{\mathrm{B}}T}\right)}, \quad (26)$$

$$g^{>(<)}_{\mathrm{s}}(\omega) = \frac{\exp\left[-\frac{(\hbar\omega)^2-\Delta^2}{(\hbar\Omega)^2}\right]}{1+\exp\left(\mp\frac{\hbar\omega}{k_{\mathrm{B}}T}\right)}\,\mathrm{Im}\,\frac{\hbar\omega+\mathrm{i}\gamma_{\mathrm{D}}\Delta}{\sqrt{\Delta^2-(\hbar\omega+\mathrm{i}\gamma_{\mathrm{D}}\Delta)^2}}. \quad (27)$$

The characteristic decay rate of the correlation functions is determined by the temperature and is equal to $k_{\mathrm{B}}T/\hbar$. This rate should sufficiently exceed the relaxation rate of the resonator $\min(Z_{\mathrm{r}}, R_{\mathrm{K}})\omega_{\mathrm{r}}/R_{\mathrm{j}}$, which introduces a restriction on the temperature at which the above-utilized Born–Markov approximation is valid.

Instead of solving Eq. (15), we simplify it further by applying a so-called secular approximation to the master equation, leaving only the terms that do not quickly oscillate in time in the interaction picture. As the first step of this simplification, we express the Redfield master Eq. (15) as

$$\frac{\mathrm{d}\hat{\rho}}{\mathrm{dt}} = -\mathrm{i}\omega_\mathrm{r}\left[\hat{a}^\dagger\hat{a},\hat{\rho}\right] - \left(\hat{F}\hat{F}_1^\dagger\hat{\rho} - \hat{F}_1^\dagger\hat{\rho}\hat{F} + \hat{\rho}\hat{F}_2^\dagger\hat{F} - \hat{F}\hat{\rho}\hat{F}_2^\dagger + \hat{F}^\dagger\hat{F}_2\hat{\rho} - \hat{F}_2\hat{\rho}\hat{F}^\dagger + \hat{\rho}\hat{F}_1\hat{F}^\dagger - \hat{F}^\dagger\hat{\rho}\hat{F}_1\right), \tag{28}$$

where

$$\hat{F}_1 = \frac{1}{\hbar^2}\int_0^{+\infty}\hat{F}(-\tau)\left\langle\hat{\Theta}^\dagger\hat{\Theta}(\tau)\right\rangle d\tau, \tag{29}$$

$$\hat{F}_2 = \frac{1}{\hbar^2}\int_0^{+\infty}\hat{F}(-\tau)\left\langle\hat{\Theta}(\tau)\hat{\Theta}^\dagger\right\rangle d\tau. \tag{30}$$

Next, we move to the frame rotating with the bare oscillator frequency ω_r such that

$$\hat{\rho}(t) = \mathrm{e}^{-\mathrm{i}\omega_\mathrm{r}t\hat{a}^\dagger\hat{a}}\tilde{\rho}(t)\mathrm{e}^{\mathrm{i}\omega_\mathrm{r}t\hat{a}^\dagger\hat{a}}. \tag{31}$$

In this frame, the density operator $\tilde{\rho}$ satisfies the following equation:

$$\frac{\mathrm{d}\tilde{\rho}}{\mathrm{dt}} = -\hat{F}(t)\hat{F}_1^\dagger(t)\tilde{\rho} + \hat{F}_1^\dagger(t)\tilde{\rho}\hat{F}(t) - \tilde{\rho}\hat{F}_2^\dagger(t)\hat{F}(t) + \hat{F}(t)\tilde{\rho}\hat{F}_2^\dagger(t) - \hat{F}^\dagger(t)\hat{F}_2(t)\tilde{\rho} + \hat{F}_2(t)\tilde{\rho}\hat{F}^\dagger(t) - \tilde{\rho}\hat{F}_1(t)\hat{F}^\dagger(t) + \hat{F}^\dagger(t)\tilde{\rho}\hat{F}_1(t), \tag{32}$$

where

$$\hat{F}(t) = \mathrm{e}^{\mathrm{i}\omega_\mathrm{r}t\hat{a}^\dagger\hat{a}}\hat{F}\mathrm{e}^{-\mathrm{i}\omega_\mathrm{r}t\hat{a}^\dagger\hat{a}}, \tag{33}$$

$$\hat{F}_1(t) = \mathrm{e}^{\mathrm{i}\omega_\mathrm{r}t\hat{a}^\dagger\hat{a}}\hat{F}_1\mathrm{e}^{-\mathrm{i}\omega_\mathrm{r}t\hat{a}^\dagger\hat{a}}, \tag{34}$$

$$\hat{F}_2(t) = \mathrm{e}^{\mathrm{i}\omega_\mathrm{r}t\hat{a}^\dagger\hat{a}}\hat{F}_2\mathrm{e}^{-\mathrm{i}\omega_\mathrm{r}t\hat{a}^\dagger\hat{a}}. \tag{35}$$

We write the equation for the matrix elements of $\tilde{\rho}_{mn} = \langle m|\tilde{\rho}|n\rangle$ in the basis of the eigenfunctions of the harmonic oscillator as follows:

$$\begin{aligned}\frac{\mathrm{d}\tilde{\rho}_{mn}}{\mathrm{d}t} = \sum_{pq}\Big[&F_{1mp}^\dagger\tilde{\rho}_{pq}F_{qn}\mathrm{e}^{\mathrm{i}\omega_\mathrm{r}(m-p+q-n)t} \\ &- F_{mp}F_{1pq}^\dagger\tilde{\rho}_{qn}\mathrm{e}^{\mathrm{i}\omega_\mathrm{r}(m-q)t} + F_{mp}\tilde{\rho}_{pq}F_{2qn}^\dagger\mathrm{e}^{\mathrm{i}\omega_\mathrm{r}(m-p+q-n)t} \\ &- \tilde{\rho}_{mp}F_{2pq}^\dagger F_{qn}\mathrm{e}^{\mathrm{i}\omega_\mathrm{r}(p-n)t} + F_{2mp}\tilde{\rho}_{pq}F_{qn}^\dagger\mathrm{e}^{\mathrm{i}\omega_\mathrm{r}(m-p+q-n)t} \\ &- F_{mp}^\dagger F_{2pq}\tilde{\rho}_{qn}\mathrm{e}^{\mathrm{i}\omega_\mathrm{r}(m-q)t} + F_{mp}^\dagger\tilde{\rho}_{pq}F_{1qn}\mathrm{e}^{\mathrm{i}\omega_\mathrm{r}(m-p+q-n)t} \\ &- \tilde{\rho}_{mp}F_{1pq}F_{qn}^\dagger\mathrm{e}^{\mathrm{i}\omega_\mathrm{r}(p-n)t}\Big],\end{aligned} \tag{36}$$

where

$$F_{mn} = \langle m|\hat{F}|n\rangle,\ F_{mn}^\dagger = \langle m|\hat{F}^\dagger|n\rangle, \tag{37}$$

$$F_{1mn} = \langle m|\hat{F}_1|n\rangle,\ F_{1mn}^\dagger = \langle m|\hat{F}_1^\dagger|n\rangle, \tag{38}$$

$$F_{2mn} = \langle m|\hat{F}_2|n\rangle,\ F_{2mn}^\dagger = \langle m|\hat{F}_2^\dagger|n\rangle. \tag{39}$$

In the secular approximation, we drop the terms that quickly oscillate in the rotating frame, leaving only slowly changing. This is justified if the characteristic decay rate $\min(Z_\mathrm{r}, R_\mathrm{K})/R_\mathrm{j}\omega_\mathrm{r}$ lies well below the bare resonator frequency ω_r. Finally, we obtain the Lindblad equation for the resonator density operator,

$$\begin{aligned}\frac{\mathrm{d}\tilde{\rho}_{mn}}{\mathrm{dt}} = \sum_p\Big\{&\tilde{\rho}_{p(p+n-m)}\Big[F_{1mp}^\dagger F_{(p+n-m)n} + F_{mp}F_{2(p+n-m)n}^\dagger \\ &+ F_{2mp}F_{(p+n-m)n}^\dagger + F_{mp}^\dagger F_{1(p+n-m)n}\Big] - \tilde{\rho}_{mn} \\ &\times\left[F_{mp}F_{1\ \mathrm{pm}}^\dagger + F_{2np}^\dagger F_{pn} + F_{mp}^\dagger F_{2\ \mathrm{pm}} + F_{1np}F_{pn}^\dagger\right]\Big\}.\end{aligned} \tag{40}$$

Note that the system of equations can be separated into a set of independent systems, which couple only matrix elements $\tilde{\rho}_{mn}$ with fixed $m - n$. This observation significantly reduces the computational resources required for the calculations. We refer to the Liouvillian of the Lindblad master equation as $\mathscr{L}_\mathrm{sec}$.

The steady-state density operator of the resonator satisfies $\mathscr{L}_\mathrm{sec}(\hat{\rho}_0) = 0$. Using the master equation, we calculate the response function $D(\omega)$ with respect to an infinitesimal drive[30–33] proportional to $\hat{a} + \hat{a}^\dagger$,

$$D(\omega) = -\mathrm{i}\,\mathrm{Tr}\left\{\left(\hat{a} + \hat{a}^\dagger\right)(\mathscr{L}_\mathrm{sec} + \mathrm{i}\omega)^{-1}\left[\hat{a} + \hat{a}^\dagger, \hat{\rho}_0\right]\right\}. \tag{41}$$

For an isolated resonator in its ground state, the response function equals

$$D_0(\omega) = \frac{2\omega_\mathrm{r}}{\omega_\mathrm{r}^2 - (\omega + \mathrm{i}0)^2}. \tag{42}$$

The poles of the response function as functions of the complex-valued frequency ω define the characteristic frequencies and decay rates of the modes in the system. From the definition of $D(\omega)$, we observe that these poles correspond to the eigenvalues λ_j of the secular Liouvillian $\mathscr{L}_\mathrm{sec}$. Accordingly, the general response function can be expanded as

$$D(\omega) = \sum_j\frac{f_j}{\lambda_j + \mathrm{i}\omega}, \tag{43}$$

where the real and imaginary parts of λ_j give the decay rate and frequency of the jth transition, respectively. The complex amplitude f_j quantifies how much this transition contributes to the response function.

Figure 3 shows the dissipation rate and the frequency shift of the resonator as functions of the dc voltage applied to the NIS junction, obtained from eigenvalues of the Liouvillian of the master equation. Here, we study a high-impedance resonator with $Z_\mathrm{r} = 20$ kΩ, and consequently increased the junction resistance to $R_\mathrm{j} = 640$ kΩ in order to work in the validity regime of the Born–Markov theory. In contrast to the low-impedance case, we observe here several resonances that differ in frequency and decay rate. Lowering the temperature to $T = 0.02$ K significantly increases the number of pronounced branches. We suggest that these branches correspond to the multi-photon transitions in the resonator, similar to those found in Ref. 34. If the voltage is $eV_0 \approx \Delta - \hbar\omega_\mathrm{r}n$, where n is a positive integer, then tunneling processes with absorption of n and more photons from the resonator are allowed. This implies that the resonator states with n or more photons rapidly decay to lower-energy states, while states with less than n photons decay relatively slowly. Thus, the system relaxes to some non-equilibrium steady state with almost zero probability of having n or more photons,

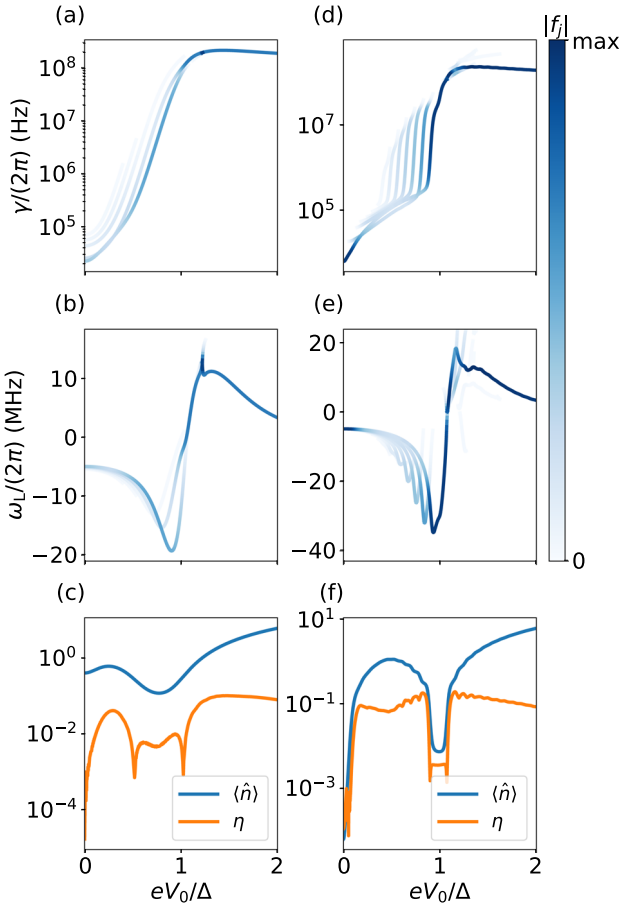

FIG. 3. (a) QCR-induced dissipation rate, (b) frequency shift, and (c) the mean photon number $\langle\hat{n}\rangle$ and the distance to the closest thermal state η defined in Eq. (44) for a high-impedance resonator as a function of the dc voltage across the NIS junction. The parameters are given by $\omega_r = 2\pi \times 4.67$ GHz, $Z_r = 20$ kΩ, $\Delta = 0.215$ meV, $T = 0.17$ K, $\gamma_D = 4 \times 10^{-4}$, and $R_j = 640$ kΩ. (d)–(f) As panels (a)–(c) except for $T = 0.02$ K. The color of the lines in the panels (a), (b), (d), and (e) corresponds to the relative absolute value of f_j, which quantifies the contribution of the resonance to the response function $D(\omega)$.

whereas the lower-energy states may have non-negligible occupation. If $n = 1$, the QCR absorbs all photons from the resonator and the system relaxes toward the ground state. At negative n (voltages above Δ/e), photon emission processes come into play and we effectively heat the system. However, due to the complicated nonlinear interaction between the resonator and the QCR, the photon distribution remains non-thermal.

To confirm this qualitative picture, we calculate two static properties of the steady state: the mean occupation number, $\langle\hat{n}\rangle = \mathrm{Tr}\{\hat{\rho}_0 \hat{a}^\dagger \hat{a}\}$, and trace distance to the closest thermal state,[35]

$$\eta = \inf_\beta \left\| \hat{\rho}_0 - \left(1 - e^{-\beta}\right) e^{-\beta \hat{a}^\dagger \hat{a}} \right\|, \tag{44}$$

where $\|\hat{A}\| = \mathrm{Tr}\{\sqrt{\hat{A}\hat{A}^\dagger}\}$. These quantities are shown in Figs. 3(c) and 3(f) as functions of the bias voltage V_0. At very low voltages, the system is in a thermal state; hence, η is very low and $\langle\hat{n}\rangle$ corresponds to the thermal distribution with temperature T. With increasing voltage, the resonator heats up due to the finite Dynes parameter of the superconductor and weak tunneling to the subgap states. When approaching the voltage $eV_0 \sim \Delta$, the occupation number decreases and so does the distance to the thermal state, since the single-photon processes come into play. This effect is especially pronounced in the low-temperature case shown in Fig. 3(f), where a sudden drop almost to the ground state in the interval $\Delta - \hbar\omega_r < eV_0 < \Delta + \hbar\omega_r$ is visible. With a further voltage increase, photon emission comes into play and the QCR starts to heat the resonator. Remarkably, the steady state in this regime still remains non-thermal for high-characteristic-impedance resonators.

V. CONCLUSIONS

To summarize, in this paper, we have proposed a simple design of a QCR consisting of a single NIS junction directly connected to the cooling system. We showed that the QCR-induced dissipation rate and the frequency shift of the low-characteristic-impedance resonator can be found from a semiclassical treatment of the dynamics of the electromagnetic field in the circuit. To study the high-characteristic-impedance resonators and to obtain a distribution of photons in the steady state, we employed the Born–Markov master equation approach to the resonator dynamics. We calculated the response function, the poles of which give the characteristic frequencies and decay rates of the resonator. We showed that a single bright resonance of the response function for the low-characteristic-impedance resonators splits into several resonances for the high-characteristic-impedance resonators, which correspond to the transitions between the shifted consecutive levels of the resonator. The short decay time of the high-energy levels due to the multi-photon transitions present in this system leads to a significant broadening of some of the transitions. We also calculated the mean photon number and the distance between the steady state to the closest thermal state. We showed that for the high-characteristic-impedance resonators, the photon distribution function is essentially non-thermal due to the multi-photon transitions. With this single-junction device, we can achieve all the desired functionalities of a double-junction QCR. It can be used as a platform for studying open quantum systems, which exhibit nontrivial phenomena in the non-linear limit.

ACKNOWLEDGMENTS

We thank Alexander Mel'nikov, Sergei Sharov, Dmitry Golubev, Gianluigi Catelani, and Matti Silveri for useful discussions. This work was financially supported by the European Research Council under Grant Nos. 681311 (QUESS) and 957440 (SCAR), the Academy of Finland under Grant No. 318937 and under its Centres of Excellence Program (Project Nos. 312300 and 312298), and the Finnish Cultural Foundation. We acknowledge the computational resources provided by the Aalto Science-IT project.

AUTHOR DECLARATIONS

Conflict of Interest

The authors have no conflicts to disclose.

Author Contributions

V. Vadimov: Formal analysis (equal); Investigation (equal); Visualization (equal); Writing – original draft (equal); Writing – review & editing (equal). **A. Viitanen:** Visualization (equal); Writing – original draft (equal); Writing – review & editing (equal). **T. Mörstedt:** Writing – original draft (equal); Writing – review & editing (equal). **T. Ala-Nissila:** Supervision (equal); Writing – original draft (equal); Writing – review & editing (equal). **M. Möttönen:** Conceptualization (equal); Supervision (equal); Writing – original draft (equal); Writing – review & editing (equal).

DATA AVAILABILITY

Data sharing is not applicable to this article as no new data were created or analyzed in this study.

REFERENCES

[1] Y. Nakamura, Y. A. Pashkin, and J. S. Tsai, "Coherent control of macroscopic quantum states in a single-cooper-pair box," Nature **398**, 786–788 (1999).

[2] A. Wallraff, D. I. Schuster, A. Blais, L. Frunzio, R. S. Huang, J. Majer, S. Kumar, S. M. Girvin, and R. J. Schoelkopf, "Strong coupling of a single photon to a superconducting qubit using circuit quantum electrodynamics," Nature **431**, 162–167 (2004).

[3] P. Krantz, M. Kjaergaard, F. Yan, T. P. Orlando, S. Gustavsson, and W. D. Oliver, "A quantum engineer's guide to superconducting qubits," Appl. Phys. Rev. **6**, 021318 (2019).

[4] A. Blais, A. L. Grimsmo, S. M. Girvin, and A. Wallraff, "Circuit quantum electrodynamics," Rev. Mod. Phys. **93**, 025005 (2021).

[5] M. Partanen, K. Y. Tan, J. Govenius, R. E. Lake, M. K. Mäkelä, T. Tanttu, and M. Möttönen, "Quantum-limited heat conduction over macroscopic distances," Nat. Phys. **12**, 460–464 (2016).

[6] V. A. Sevriuk, K. Y. Tan, E. Hyyppä, M. Silveri, M. Partanen, M. Jenei, S. Masuda, J. Goetz, V. Vesterinen, L. Grönberg, and M. Möttönen, "Fast control of dissipation in a superconducting resonator," Appl. Phys. Lett. **115**, 082601 (2019).

[7] H. Hsu, M. Silveri, A. Gunyhó, J. Goetz, G. Catelani, and M. Möttönen, "Tunable refrigerator for nonlinear quantum electric circuits," Phys. Rev. B **101**, 235422 (2020).

[8] T. Yoshioka and J. S. Tsai, "Fast unconditional initialization for superconducting qubit and resonator using quantum-circuit refrigerator," Appl. Phys. Lett. **119**, 124003 (2021).

[9] D. Basilewitsch, J. Fischer, D. M. Reich, D. Sugny, and C. P. Koch, "Fundamental bounds on qubit reset," Phys. Rev. Res. **3**, 013110 (2021).

[10] P. Magnard, P. Kurpiers, B. Royer, T. Walter, J. C. Besse, S. Gasparinetti, M. Pechal, J. Heinsoo, S. Storz, A. Blais, and A. Wallraff, "Fast and unconditional all-microwave reset of a superconducting qubit," Phys. Rev. Lett. **121**, 060502 (2018).

[11] K. Geerlings, Z. Leghtas, I. M. Pop, S. Shankar, L. Frunzio, R. J. Schoelkopf, M. Mirrahimi, and M. H. Devoret, "Demonstrating a driven reset protocol for a superconducting qubit," Phys. Rev. Lett. **110**, 120501 (2013).

[12] K. Y. Tan, M. Partanen, R. E. Lake, J. Govenius, S. Masuda, and M. Möttönen, "Quantum-circuit refrigerator," Nat. Commun. **8**, 15189 (2017).

[13] T. F. Mörstedt, A. Viitanen, V. Vadimov, V. Sevriuk, M. Partanen, E. Hyyppä, G. Catelani, M. Silveri, K. Y. Tan, and M. Möttönen, "Recent developments in quantum-circuit refrigeration," Ann. Phys. (Berlin) (published online 2022).

[14] M. Silveri, H. Grabert, S. Masuda, K. Y. Tan, and M. Möttönen, "Theory of quantum-circuit refrigeration by photon-assisted electron tunneling," Phys. Rev. B **96**, 094524 (2017).

[15] F. Giazotto, T. T. Heikkilä, A. Luukanen, A. M. Savin, and J. P. Pekola, "Opportunities for mesoscopics in thermometry and refrigeration: Physics and applications," Rev. Mod. Phys. **78**, 217–274 (2006).

[16] L. Kuzmin, A. Pankratov, A. Gordeeva, V. Zbrozhek, V. Shamporov, L. Revin, A. Blagodatkin, S. Masi, and P. de Bernardis, "Photon-noise-limited cold-electron bolometer based on strong electron self-cooling for high-performance cosmology missions," Commun. Phys. **2**, 104 (2019).

[17] H. Q. Nguyen, T. Aref, V. J. Kauppila, M. Meschke, C. B. Winkelmann, H. Courtois, and J. P. Pekola, "Trapping hot quasi-particles in a high-power superconducting electronic cooler," New J. Phys. **15**, 085013 (2013).

[18] J. Pekola, R. Schoelkopf, J. Ullom *et al.*, "Cryogenics on a chip," Phys. Today **57**, 41–47 (2004).

[19] J. T. Muhonen, M. Meschke, and J. P. Pekola, Rep. Prog. Phys. **75**, 046501 (2012).

[20] A. Bardas and D. Averin, "Peltier effect in normal-metal–superconductor microcontacts," Phys. Rev. B **52**, 12873–12877 (1995).

[21] H. Courtois, F. W. J. Hekking, H. Q. Nguyen, and C. B. Winkelmann, "Electronic coolers based on superconducting tunnel junctions: Fundamentals and applications," J. Low Temp. Phys. **175**, 799–812 (2014).

[22] P. J. Lowell, G. C. O'Neil, J. M. Underwood, and J. N. Ullom, "Macroscale refrigeration by nanoscale electron transport," Appl. Phys. Lett. **102**, 082601 (2013).

[23] G.-L. Ingold and Y. V. Nazarov, "Charge tunneling rates in ultrasmall junctions," in *Single Charge Tunneling* (Springer, 1992), pp. 21–107.

[24] S. Masuda, K. Y. Tan, M. Partanen, R. E. Lake, J. Govenius, M. Silveri, H. Grabert, and M. Möttönen, "Observation of microwave absorption and emission from incoherent electron tunneling through a normal-metal–insulator –superconductor junction," Sci. Rep. **8**, 3966 (2018).

[25] E. Hyyppä, M. Jenei, S. Masuda, V. Sevriuk, K. Y. Tan, M. Silveri, J. Goetz, M. Partanen, R. E. Lake, L. Grönberg, and M. Möttönen, "Calibration of cryogenic amplification chains using normal-metal–insulator–superconductor junctions," Appl. Phys. Lett. **114**, 192603 (2019).

[26] H. Hsu, M. Silveri, V. Sevriuk, M. Möttönen, and G. Catelani, "Charge dynamics in quantum-circuit refrigeration: Thermalization and microwave gain," AVS Quantum Sci. **3**, 042001 (2021).

[27] M. Silveri, S. Masuda, V. Sevriuk, K. Y. Tan, M. Jenei, E. Hyyppä, F. Hassler, M. Partanen, J. Goetz, R. E. Lake *et al.*, "Broadband lamb shift in an engineered quantum system," Nat. Phys. **15**, 533–537 (2019).

[28] J. R. Tucker and M. J. Feldman, "Quantum detection at millimeter wavelengths," Rev. Mod. Phys. **57**, 1055 (1985).

[29] A. G. Redfield, "The theory of relaxation processes," in *Advances in Magnetic and Optical Resonance* (Elsevier, 1965), Vol. 1, pp. 1–32.

[30] V. V. Albert, B. Bradlyn, M. Fraas, and L. Jiang, "Geometry and response of lindbladians," Phys. Rev. X **6**, 041031 (2016).

[31] M. Ban, "Linear response theory for open quantum systems within the framework of the abl formalism," Quantum Stud.: Math. Found. **2**, 51–62 (2015).

[32] L. Campos Venuti and P. Zanardi, "Dynamical response theory for driven-dissipative quantum systems," Phys. Rev. A **93**, 032101 (2016).

[33] B. Villegas-Martínez, F. Soto-Eguibar, and H. Moya-Cessa, "Application of perturbation theory to a master equation," Adv. Math. Phys. **2016**, 9265039.

[34] A. Viitanen, M. Silveri, M. Jenei, V. Sevriuk, K. Y. Tan, M. Partanen, J. Goetz, L. Grönberg, V. Vadimov, V. Lahtinen, and M. Möttönen, "Photon-number-dependent effective lamb shift," Phys. Rev. Res. **3**, 033126 (2021).

[35] M. Hillery, "Nonclassical distance in quantum optics," Phys. Rev. A **35**, 725–732 (1987).